



Nanofiltration membrane via EGCG-PEI co-deposition followed by cross-linking on microporous PTFE substrates for desalination



Na Zhang, Zhaohu Huang, Na Yang*, Luhong Zhang, Bin Jiang, Yongli Sun, Jingwen Ma

School of Chemical Engineering and Technology, Tianjin University, Tianjin 300072, PR China

ARTICLE INFO

Keywords:

Nanofiltration
Polyphenol-inspired coating
Cross-linking
Desalination
Dye removal

ABSTRACT

It is imperative to fabricate nanofiltration membrane with promising separation performance and stability for desalination and wastewater treatment. In this work, inspired by polyphenol chemistry, composite nanofiltration membrane is facilely manufactured by a combined strategy of epigallocatechin-3-gallate (EGCG)-polyethylenimine (PEI) co-deposition and trimesoyl chloride (TMC) cross-linking on porous polytetrafluoroethylene (PTFE) substrate. Separation performance of membrane was optimized by controlling EGCG-PEI coating time, EGCG-PEI mass ratio and TMC concentration. Chemical structures and surface properties of the optimal membrane were characterized systematically. It was found that a dense and defect-free selective layer was formed with negatively charged surface and molecular weight cut off of 380 Da (stokes radius of 0.46 nm). Experimental results showed that the optimal membrane yielded a pure water permeability of 9.15 L/(m²·h·bar), high rejections of salts in a sequence of Na₂SO₄ (95.5%) > MgSO₄ (86.3%) > MgCl₂ (79.1%) > NaCl (61.4%) and excellent rejections of dyes (99.9% for neutral red, methyl orange and crystal violet) at 0.2 MPa. Moreover, the membrane exhibited favorable structural stability and long-term operation stability due to the strong EGCG-PEI adhesion property and robust interfacial interactions.

1. Introduction

Water scarcity is perceived as one of the most serious worldwide challenges, as two-thirds of the global population undergo severe water shortage at least one month a year [1,2]. Among the membrane-based technologies for water treatment, nanofiltration (NF) has been of great interest and increasing significance in water desalination and wastewater reuse due to its high retention of multivalent ions and low-molecular-weight (< 1000 Da) organic molecules [3]. NF membrane is a kind of pressure-driven membrane whose separation characteristics are between those of ultrafiltration (UF) membrane and reverse osmosis (RO) membrane with advantages of relatively high separation capacity and low energy consumption [4,5]. Currently, interfacial polymerization is the dominant technique to fabricate both commercial and laboratory NF membrane which comprises a polyamide selective layer attached onto a porous substrate that is typically an ultrafiltration or a microfiltration membrane [6]. However, the compatibility between the selective layer and the support layer might not be good enough to endow the membrane satisfactory structural stability in harsh conditions [7], as there's no chemical bonding force between these two layers. To ensure the structural integrity of composite NF membrane and confer attractive properties to the selective layer, surface coating

with advanced functional building blocks followed by in-situ cross-linking on porous substrate is proved to be an effective strategy [8,9].

Dopamine (DA), a kind of catecholamine, has been verified to be self-polymerized spontaneously under aerobic and weak alkaline conditions and form adhesive and functional coatings on various substrates [10]. In the past decade, numerical studies have applied mussel-inspired coatings to fabricate composite NF membranes [7,11–14]. Despite of these inspiring studies, DA might encounter with drawbacks in its practical application. It is susceptible to deterioration in storage due to the coexistence of catechol and amine groups within one molecule [15]. Besides, the dark color of the formed coatings further set limit on its applicability. In this regard, it is desired to develop alternative coating strategies for fabricating versatile membranes.

Plant polyphenols with high content of catechol/pyrogallol groups have been verified to form multifunctional coatings ascribed to the oxidative oligomerization of polyphenol precursors under mild conditions as reported by Messersmith and co-workers [16]. They show great potentials as green building blocks for material engineering, such as modification of hydrogels [17], capsules [18], thin films and particles [19]. In addition, polyphenol-inspired coatings not only retain the merits of PDA coatings, but also exhibit better stability and light colors [20]. Recently, the feasibility and superiority of employing polyphenol

* Corresponding author.

E-mail address: yangnayna@tju.edu.cn (N. Yang).

<https://doi.org/10.1016/j.seppur.2019.115964>

Received 21 May 2019; Received in revised form 19 August 2019; Accepted 19 August 2019

Available online 20 August 2019

1383-5866/ © 2019 Elsevier B.V. All rights reserved.

chemistry for developing NF membranes have been verified. Abdellah et al. successfully fabricated a novel composite organic solvent nanofiltration membrane via the interfacial polymerization of catechin and terephthaloyl chloride on cellulose porous substrate [21]. Shao's group designed a novel Ni^{2+} -polyphenol network as an excellent bio-coating to obtain NF membranes with unconventional high water flux and high rejection for rose Bengal [22]. Xu and coworkers thoroughly investigated the catechol-amine reaction occurring on the active layer of NF membrane [20]. Nonetheless, the utilization of polyphenol-inspired coating strategy for fabricating NF membrane has not yet been extensively explored. There's still great room for further investigation. Epigallocatechin gallate (EGCG) is the most abundant natural polyphenol in green tea. And it is more available and less expensive than other green tea catechins such as epicatechin, epicatechin gallate and epigallocatechin (chemical structures of green tea catechins are shown in Fig. S1). Previously, we found that EGCG could deposit with polyethyleneimine (PEI, a commercially available polymer with abundant amino groups) on membrane surface to form a hydrophilic and robust selective layer by means of Michael addition/Schiff base reaction and non-covalent interactions [23]. However, the as-prepared loose NF membranes were aimed to separate dyes and salts in textile wastewater rather than to desalinate water. Herein, EGCG involved coatings were further employed to fabricate dense NF membranes by a combined strategy of surface coating and cross-linking for water softening and remediation.

In this work, we proposed a straightforward and effective method to fabricate dense NF membranes for inorganic salt and dye removal via the co-deposition of EGCG-PEI followed with cross-linking by trimesoyl chloride (TMC) onto hydrophilic microporous polytetrafluoroethylene (PTFE) substrate. The chemical structures, morphologies, hydrophilicity and charge properties of the resultant membranes were systematically studied. Effects of EGCG-PEI coating time, EGCG-PEI mass ratio and TMC concentration on membrane separation performance were also evaluated to obtain the optimal membrane. Moreover, the separation efficiency towards different inorganic salts and relative low-molecular-weight dyes along with the structural stability in ethanol and long-term performance stability of the optimal membrane were assessed. This work would offer useful insights into the designing of dense NF membranes on basis of polyphenol chemistry for water softening and recycling.

2. Experimental

2.1. Materials

Porous PTFE (both hydrophilic and hydrophobic, pore size: 0.22 μm), polyethersulfone (PES, pore size: 0.22 μm) and polyvinylidene fluoride (PVDF, pore size: 0.1 μm and 0.22 μm) membranes with diameter of 100 mm were supplied by Haining Zhongli Filtering Equipment Factory (China). Epigallocatechin-3-gallate (EGCG, >95%) was purchased from Dalian Meilun Biological Technology Co., Ltd. (China). Bicine (99%) was purchased from Tianjin Heowns Biochem LLC (China). Branched polyethyleneimine (PEI, 99%, $M_w = 1800$) was provided by Shanghai Macklin Biochemical Co., Ltd. (China). Trimesoyl chloride (TMC, 99%) was purchased from J&K LLC (China). NaCl (98.0%), MgCl_2 (98.0%), Na_2SO_4 (99.0%), MgSO_4 (99.5%), NaOH (98.0%), diethylene glycol, polyethylene glycol (PEG, with different molecular weights 200, 400, 600, 1000), ethanol and n-hexane were supplied by Tianjin Kermel Chemical Reagent Co., Ltd. (China). Neutral red, methyl orange and crystal violet were purchased from Tianjin Yuanli Chemical Co., Ltd. (China). The basic properties of dyes are shown in Table 1. The water used in the experiments was deionized (DI) water.

2.2. Fabrication of composite NF membranes

Prior to surface coating, hydrophilic PTFE substrates were immersed in DI water for 4 h then thoroughly washed with DI water. The coating solutions were prepared by dissolving EGCG at a fixed concentration of 0.5 mg/mL and PEI at certain concentrations in buffered saline (pH 7.8). Then, PTFE substrates were immersed in the above coating solution for certain time in air at ambient temperature. Notably, only top surfaces of PTFE membranes were exposed to the coating solutions in a home-made device (see Fig. S2). Subsequently, the coated membranes were washed thoroughly with DI water to remove unreacted chemicals. After dried by filter paper, the top surfaces of membranes were immersed into TMC solution (dissolved in n-hexane) for further cross-linking at 60 °C for 20 min. Then, the membranes were thoroughly washed with n-hexane to remove residual chemicals followed by post-treatment in vacuum at 60 °C for 20 min. As a control, NF membranes were also fabricated via direct interfacial polymerization of PEI and TMC on PTFE substrates. Finally, the resultant NF membranes were rinsed several times and preserved in DI water overnight before characterization and evaluation. The surface modification strategy was also applied to fabricate other composite NF membranes with porous PES, PVDF and hydrophobic PTFE membranes as substrates.

2.3. Membrane characterization

All membrane samples were dried under vacuum at 40 °C for 24 h prior to characterization. Attenuated total reflectance Fourier transform infrared (FTIR/ATR) spectroscopy (Bruker, Germany) analyzed the chemical structures of membrane surfaces, while X-ray photoelectron spectroscopy (XPS, Thermo, USA) characterized the compositions of membrane surfaces. Membrane surface morphology was captured by a field emission scanning electron microscopy (FESEM, Hitachi, S-4800, Japan). Membrane surface roughness in terms of average roughness (R_a) and root mean square roughness (R_q) was measured by an atom force microscopy (AFM, NTEGRA Spectra, Russia). Water contact angles of membrane samples were measured by a goniometer (Powereach, JC 2000, China) at room temperature. Zeta potential of membranes over a pH range of 3–9 was analyzed by an electrokinetic analyzer (Anton Paar SurPASS 3, Austria) with 0.001 M KCl aqueous solution.

2.4. Evaluation of membrane separation performance

The molecular weight cut off (MWCO) of NF membrane was determined by filtrating a series of neutral organic solutes (diethylene glycol and PEG, 50 mg/L) with molecular weights ranging from 106 to 1000 Da at 0.2 MPa [24]. MWCO was obtained according to the molecular weight where the rejection is 90%. A total organic carbon analyzer (TOC-L, SHIMADZU, Japan) was utilized to measure the concentration of organic solute in the feed and permeate solution. Stokes radius of neutral molecule can be calculated according to its average molecular weight based on the following equation [25]:

$$r_p = 16.73 \times 10^{-12} \times M^{0.557} \quad (1)$$

where M and r_p are the molecular weight of solute and the Stokes radius, respectively.

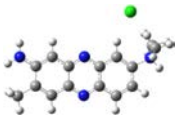
Separation performance of NF membrane was evaluated by a laboratory dead-end filtration cell (effective area of 33.18 cm^2) under 0.2 MPa at 25 °C. The membranes were pre-compacted with DI water under 0.25 MPa to reach a steady flux. Water flux (J , $\text{L}/\text{m}^2\text{h}$) of membranes was calculated by the following equation:

$$J = \frac{V}{A \cdot \Delta t} \quad (2)$$

where V , A and Δt stand for the volume of permeate (L), the effective membrane area (m^2) and the operation time interval (h), respectively.

Rejection performance of NF membrane was determined using

Table 1
Properties of dyes used in the experiments.

Dye	Molecular weight (g mol ⁻¹)	Molecular volume ^a (cm ⁻³ mol ⁻¹)	Diameter ^a (nm)	Charge	Optimized structure ^a
Neutral red	288.8	277.43	1.24	Positive	
Methyl orange	327.3	176.65	1.48	Negative	
Crystal violet	408.0	348.67	1.39	Positive	

^a Data were given by the Gaussian 09 program at the B3LYP/6-311G++ (d, p) level.

1000 mg/L salt (NaCl, Na₂SO₄, MgCl₂, and MgSO₄) solutions and 100 mg/L dye (natural red, methyl orange and crystal violet) solutions. Rejection (R, %) for salts and dyes was calculated by Eq. (3):

$$R = \left(1 - \frac{C_p}{C_f}\right) \times 100 \quad (3)$$

where C_p and C_f are the solute concentrations in the permeate and feed, respectively. The concentrations of salt solutions and dye solutions were measured with a conductivity meter (DDS-307A, Leici, China) and a UV-vis spectrophotometer (UV-4802S, Unico, USA), respectively. All results presented were repeated at least three times to ensure the reproducibility.

2.5. Membrane stability tests

The fabricated composite NF membranes were immersed into absolute ethanol for two weeks to study the structural stability. After a certain time of immersion (every 48 h), the membranes were taken out and washed thoroughly with deionized water. Then, the water flux and rejections for Na₂SO₄ and neutral red were tested again.

To evaluate membrane long-term operation stability, the composite NF membrane was tested continuously for 120 h at 0.2 MPa with 1000 mg/L Na₂SO₄ solution. The permeate flux and rejection of Na₂SO₄ were recorded every 12 h.

3. Results and discussion

3.1. Chemical structures of the membrane surfaces

Fig. 1 schematically illustrates the fabrication process of the dense NF membrane. First, EGCG-PEI coating was formed on hydrophilic microporous PTFE substrate and the resultant membrane was denominated as EGCG-PEI/PTFE. Then, the top layer was further densified by in-situ cross-linking between TMC and PEI. The final membrane was denoted as EGCG-PEI-TMC/PTFE. Additionally, the chemical structures of EGCG, PEI and TMC coupled with the possible reactions occurring on the top layer are delineated in Fig. 1.

To reveal the reaction between EGCG and PEI, UV-vis analysis was performed to monitor the absorbance of EGCG-PEI coating solution. As a control, the absorbance spectra of sole EGCG (at neutral pH) and PEI in buffered saline are also presented. As shown in Fig. 2(a), the characteristic absorption peak of EGCG at 273 nm is observed for sole EGCG solution. For EGCG-PEI solution, the emerged peak at 328 nm accounts

for the absorption of quinone structures [20,28], suggesting that the pyrogallol-type phenols in EGCG can be oxidized into quinonoid species under weak alkaline solution. The peak at around 450 nm might be attributed to the cross-linked structures between quinone and amine groups.

ATR-FTIR was applied to analyze chemical structures of the membrane surfaces. As shown in Fig. 2(b), comparing the spectra of pristine PTFE and EGCG-PEI/PTFE, the latter shows three new peaks at 1610 cm⁻¹, 1360 cm⁻¹ and 1070 cm⁻¹ corresponding to the C=C stretching vibration in the aromatic ring [29,30], C-NH-C stretching and C-O-C stretching, respectively. The results indicate the successful introduction of PEI and EGCG molecules on membrane surface. A new peak emerges on the spectrum of EGCG-PEI-TMC/PTFE at 1545 cm⁻¹ attributed to N-H stretching (amide II). Moreover, the intensity of the peak at 1610 cm⁻¹ obviously increases possibly due to the newly introduced C=C bond from TMC and N-H deformation vibration from aromatic amide [31]. The changes confirm the formation of polyamide in the active layer by cross-linking between TMC and PEI.

To further characterize the compositions of membrane surface, XPS measurement was carried out and the results are shown in Fig. 2(c) and Table 2. Of note, the spectrum of pristine PTFE contains C, F and O elements. The appearance of O element might be ascribed to the hydrophilization of PTFE. It is found that the F content declines significantly from 13.9% to 2.9% after co-deposition of EGCG-PEI on PTFE substrate, due to the surface coverage of membrane by the newly formed layer. In addition, compared to the pristine PTFE substrate, an intense signal peak of N 1s with the element content of 10.2% appears on the spectrum of the EGCG-PEI/PTFE, which is derived from PEI of the coating layer. As shown in Fig. 2(d), the high-resolution of N 1s spectrum of EGCG-PEI/PTFE presents C=N bond (at 400.4 eV), indicating that EGCG was cross-linked by amine to form Schiff base [32]. Based on the characterizations and relevant research, it can be conjectured that EGCG, similar to polydopamine, catechol and tannic acid, can be oxidized to a quinoid form and then cross-linked by the primary amine groups of PEI through a Schiff base/Michael addition reaction in an alkaline buffer solution [26,28,32-34]. After further cross-linked by TMC, both the C/N ratio and O/N ratio increase, resulting from C and O elements in TMC. Besides, the new peak at 400.0 eV on the spectrum of EGCG-PEI-TMC/PTFE (Fig. 2(d)) is assigned to O=C-N [35,36], indicating that the amidation reaction occurs between TMC and PEI. The above results demonstrate that the PTFE substrates are successfully coated by EGCG-PEI and then cross-linked by TMC.

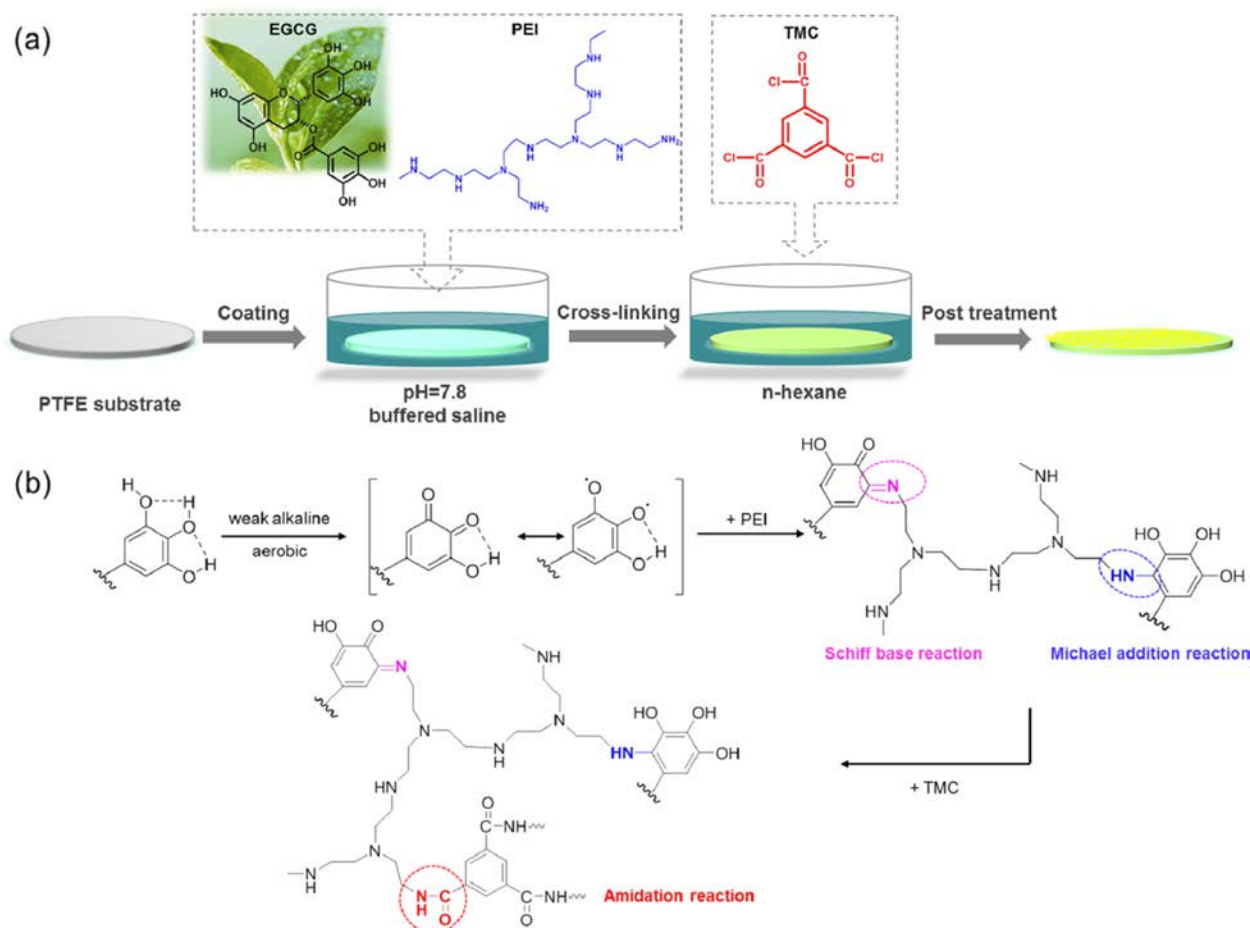


Fig. 1. (a) Fabrication process of composite NF membrane and (b) proposed reaction mechanism occurring on membrane surface [26,27].

3.2. Morphologies of the membranes

SEM served the analysis of membrane surface morphology. As shown in Fig. 3(a), pristine PTFE substrate possesses reticular microstructures consisting of fibrils connected by nodes. After the first step of EGCG-PEI co-deposition, some nano-size and micro-size aggregates formed and well-distributed on the reticular structures of membrane surface due to the adhesion property of EGCG as well as the reaction between EGCG and PEI. Consequently, the pores on the surface were partially covered. Further cross-linking by TMC generated a dense and defect-free surface layer on EGCG-PEI-TMC/PTFE, implying that polyamide was successfully formed by the cross-linking between TMC and PEI. The dense and uniform top layer, which fully covered the porous substrate without visible defects, might favor the selectivity of the composite NF membrane.

Fig. 3(b) shows the three-dimensional AFM images and the values of average roughness (R_a) and root mean square roughness (R_q) for the pristine PTFE, EGCG-PEI/PTFE and EGCG-PEI-TMC/PTFE. The R_a and R_q values of the unmodified PTFE substrate are 84.9 nm and 109.7 nm, respectively. After EGCG-PEI co-deposition, the values increase greatly to 113.1 nm and 142.4 nm, respectively, which might be attributed to the formed aggregates on membrane surface as shown in Fig. 3(a). After TMC cross-linking, the membrane surface becomes smoother with R_a and R_q values lower than those of PTFE substrate due to the coverage of substrate surface by the newly formed layer. The changes of membrane roughness correspond well to the changes of membrane morphology.

3.3. Surface properties of the membranes

Fig. 4 illustrates the static and time-dependent water contact angle (WCA) of the membranes. Due to the hydrophilic and microporous nature of the PTFE substrate, it only takes 3.5 s for WCA to decrease from 52° to 0. With EGCG-PEI coating on membrane surface, the initial WCA declines from 52° to 40°, as a result of the micro-nanostructures coupled with the abundance of hydrophilic hydroxyl and amine functional groups on membrane surface. However, the time for WCA of EGCG-PEI/PTFE to decrease to zero is longer (~8.0 s) than that of pristine PTFE, which is attributed to the reduced surface pore size as observed by SEM in Fig. 3(a). The cross-linking of amine in PEI with acyl chloride in TMC resulted in EGCG-PEI-TMC/PTFE possessing a higher contact angle (58°) due to the amide group formed by cross-linking and the hydrophobic benzene group in TMC [11]. In addition, the WCA of the membrane declines from 58° to 15° in 90 s. The relative long time is mainly caused by the dense selective layer which hinders water droplet to penetrate into membrane matrix.

Surface charge of NF membrane plays a crucial rule in the removing efficiency of charged solutes based on Donnan exclusion and dielectric effects [24,37]. Herein, the zeta potentials of EGCG-PEI coated membrane and the resultant composite NF membrane are shown in Fig. 5. It has been found that EGCG-PEI/PTFE is slightly positively-charged at pH = 6.0 as a result of the protonated amine groups ($-\text{NH}_3^+$) and its isoelectric point is about 6.68. However, the isoelectric point of EGCG-PEI-TMC/PTFE decreases dramatically to 4.71, mainly due to the hydrolysis of acyl chloride groups into carboxylic groups in the selective layer. The negatively charged surface of EGCG-PEI-TMC/PTFE at neutral and basic conditions would benefit for the separation of negatively

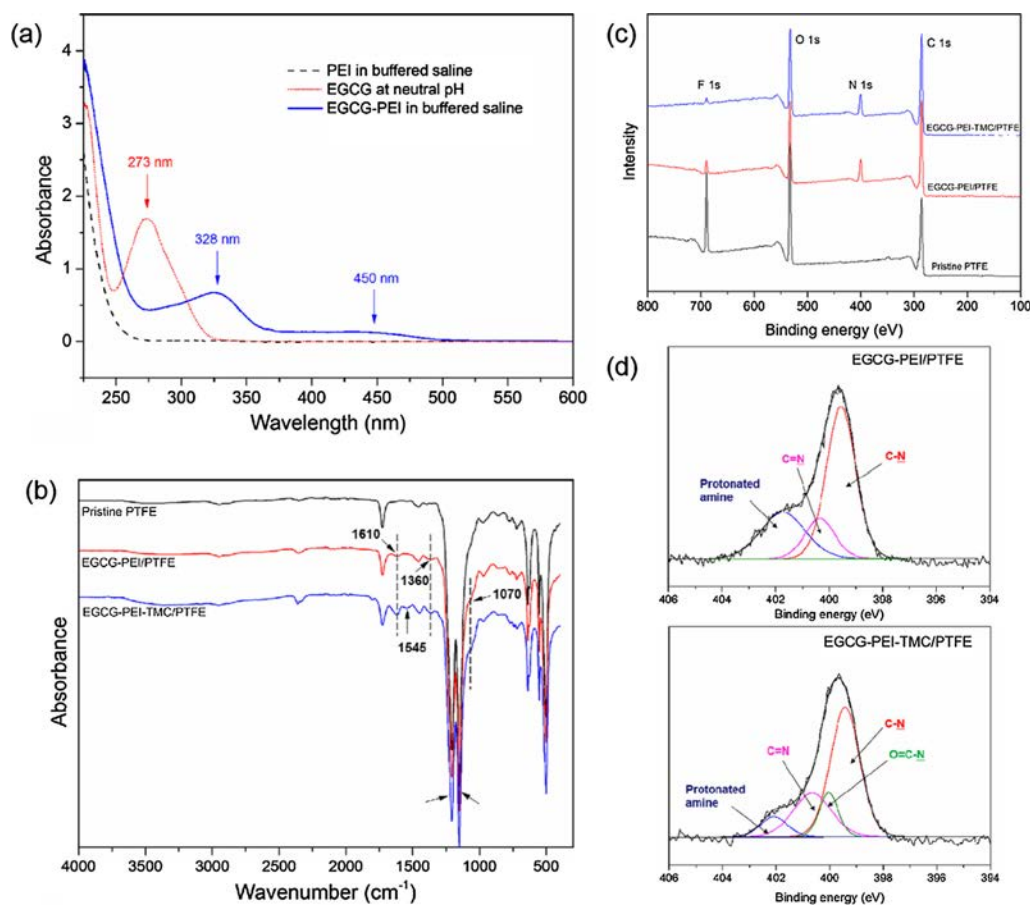


Fig. 2. (a) UV-vis spectra of 8-fold diluted sole PEI solution, sole EGCG solution, and EGCG-PEI coating solution after 6 h, (b) ATR-FTIR spectra, (c) XPS spectra of pristine PTFE, EGCG-PEI/PTFE and EGCG-PEI-TMC/PTFE and (d) de-convoluted high-resolution N 1s spectra of EGCG-PEI/PTFE and EGCG-PEI-TMC/PTFE.

charged components in solution.

3.4. Preparation condition optimization of the composite NF membranes

The effects of EGCG-PEI coating time, EGCG-PEI mass ratio and TMC concentration on the separation performance of the as-prepared composite NF membranes were investigated systematically to optimize membrane fabrication conditions. In this work, the coating time of EGCG and PEI had significant impact on membrane properties. As shown in Fig. 6(a), when the coating time increased from 0 to 6 h, the water flux decreased dramatically from 52.4 L/m²h to 9.4 L/m²h while the rejection of Na₂SO₄ increased significantly from 18.4% to 95.5%, which was ascribed to the formation of thicker and denser active layer with the prolonging of coating time. However, with the coating time further increasing, both the water flux and the rejection decreased to a small extent. It's possibly because that the coating of EGCG and PEI reached an optimum state at 6 h for the following cross-linking and membrane performance cannot be enhanced further with longer time. Similar results have also been reported in the literature [7]. Therefore, 6 h, the optimized coating time of EGCG and PEI, was chosen in the

following investigation.

The mass ratio of EGCG and PEI in the coating solution also predominantly determined the resultant membrane performance. Fig. 6(b) illustrates that as the mass ratio of EGCG and PEI increased from 1:0.5 to 1:4, the water flux decreased gradually, meanwhile the rejection of Na₂SO₄ first increases to the maximum value of 95.5% (at the mass ratio of 1:2) then decreases. The thickness and denseness variations of coating layers on porous substrates might be accounted for the results [7]. Simultaneously taking into consideration of membrane permeability and selectivity, 1:2 was the proper EGCG-PEI mass ratio for constructing NF membrane with decent performance.

Fig. 6(c) exhibits the effect of TMC concentration on the filtration performance of the composite membranes. Obviously, the rejection of Na₂SO₄ first increased from 80.3% to 95.5% with the increase of TMC concentration from 0.1 wt% to 0.2 wt% and then decreased to 71.7% as TMC concentration further increased to 1.0 wt%. Meanwhile, the water flux showed an inverse tendency. At lower TMC concentration, the degree of cross-linking on membrane surface was low ascribed to the insufficient acyl chloride groups, so that the active layer was relatively thinner and looser, leading to the lower salt rejection and higher water

Table 2

Surface elemental compositions of pristine PTFE, EGCG-PEI/PTFE and EGCG-PEI-TMC/PTFE by XPS.

Membranes	Element content (atom.%)				Element ratio	
	C 1s	F 1s	O 1s	N 1s	C/N	O/N
Pristine PTFE	59.1 ± 0.3	13.9 ± 0.4	27.0 ± 0.5			
EGCG-PEI/PTFE	65.3 ± 0.3	2.9 ± 0.1	21.6 ± 0.4	10.2 ± 0.3	6.4 ± 0.2	2.1 ± 0.0
EGCG-PEI-TMC/PTFE	66.4 ± 0.5	1.2 ± 0.2	23.2 ± 0.3	9.2 ± 0.2	7.2 ± 0.1	2.5 ± 0.0

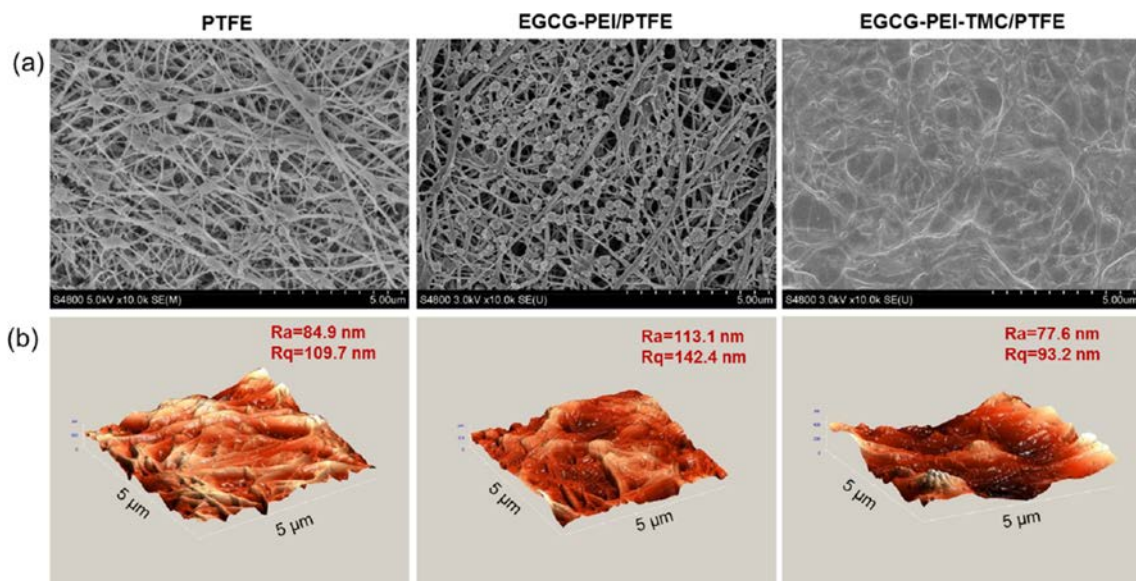


Fig. 3. (a) SEM and (b) AFM images of pristine PTFE, EGCG-PEI/PTFE and EGCG-PEI-TMC/PTFE.

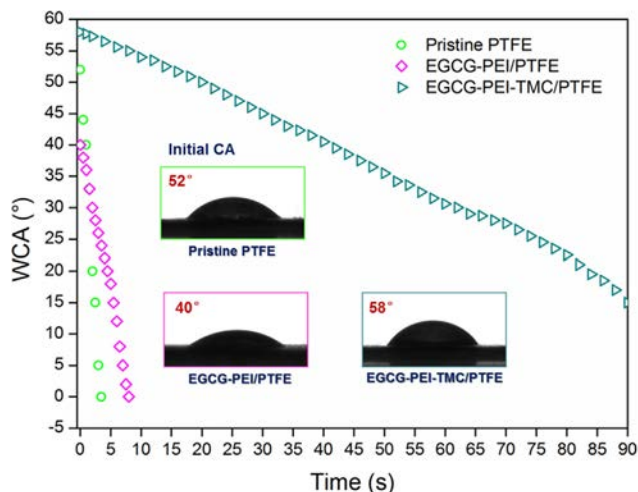


Fig. 4. Dynamic water contact angle of the membranes (the inserted pictures indicate the initial contact angle of the membranes).

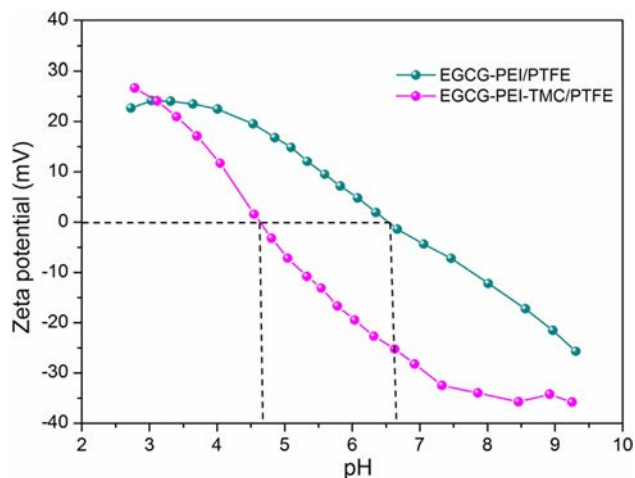


Fig. 5. Zeta potential of EGCG-PEI/PTFE and EGCG-PEI-TMC/PTFE as a function of pH.

flux. When the TMC concentration reaches to 0.2 wt%, the cross-linking reaction is the most adequate. However, at further increased TMC concentration, swelling action might occur, which caused the decreased rejection and increased water flux [38,39]. From the above, the optimized EGCG-PEI coating time, EGCG-PEI mass ratio and TMC concentration were fixed at 6 h, 1:2 and 0.2 wt%, respectively. And the NF membrane (EGCG-PEI-TMC/PTFE) prepared at the optimized conditions was employed to evaluate its potential applications in the following section.

3.5. Separation performance of the optimal EGCG-PEI-TMC/PTFE

3.5.1. MWCO and pore size

MWCO and effective surface pore size of EGCG-PEI-TMC/PTFE were determined through permeation tests to neutral organic solutes with different molecular weights. As shown in Fig. 7, as the molecular weight increases, the solute rejection of the NF membrane increases owing to the steric effect. The MWCO of EGCG-PEI-TMC/PTFE is approximately 380 Da, which corresponds to an effective pore radius of about 0.46 nm according to Eq. (1), demonstrating that the fabricated membrane falls into the category of NF membrane.

3.5.2. Pure water permeability and rejection of salts and dyes

Fig. 8 illustrates pure water flux of EGCG-PEI-TMC/PTFE membrane over operating pressure. Apparently, pure water flux increases linearly as operating pressure increases, which is well consistent with the Spiegler-Kedem model [40]. And the pure water permeability obtained from the linear fit of experiment data is 91.5 L/(m² h·MPa).

Fig. 9(a) shows the rejection of EGCG-PEI-TMC/PTFE towards four types of salt solutions. It's widely accepted that the rejection of NF membrane is mainly dominated by Donnan repulsion and steric hindrance. The negative charge on the surface of the NF membrane (shown in Fig. 5) would attract cations and repulse anions, resulting in a higher rejection to bivalent anion SO₄²⁻ while a lower rejection to bivalent cation Mg²⁺. Besides, the hydrated ionic radius follows the order of Mg²⁺ (0.43 nm) > SO₄²⁻ (0.38 nm) > Na⁺ (0.36 nm) > Cl⁻ (0.33 nm) [41]. Therefore, as a result of the synergistic effect of Donnan repulsion and size exclusion, EGCG-PEI-TMC/PTFE exhibits the following rejection order to salts: Na₂SO₄ (95.5%) > MgSO₄ (86.3%) > MgCl₂ (79.1%) > NaCl (61.4%). Fig. 9(b) shows the effect of salt concentration on membrane rejection. Apparently, the salt rejection decreases gradually from 95.5% to 83.2% with Na₂SO₄

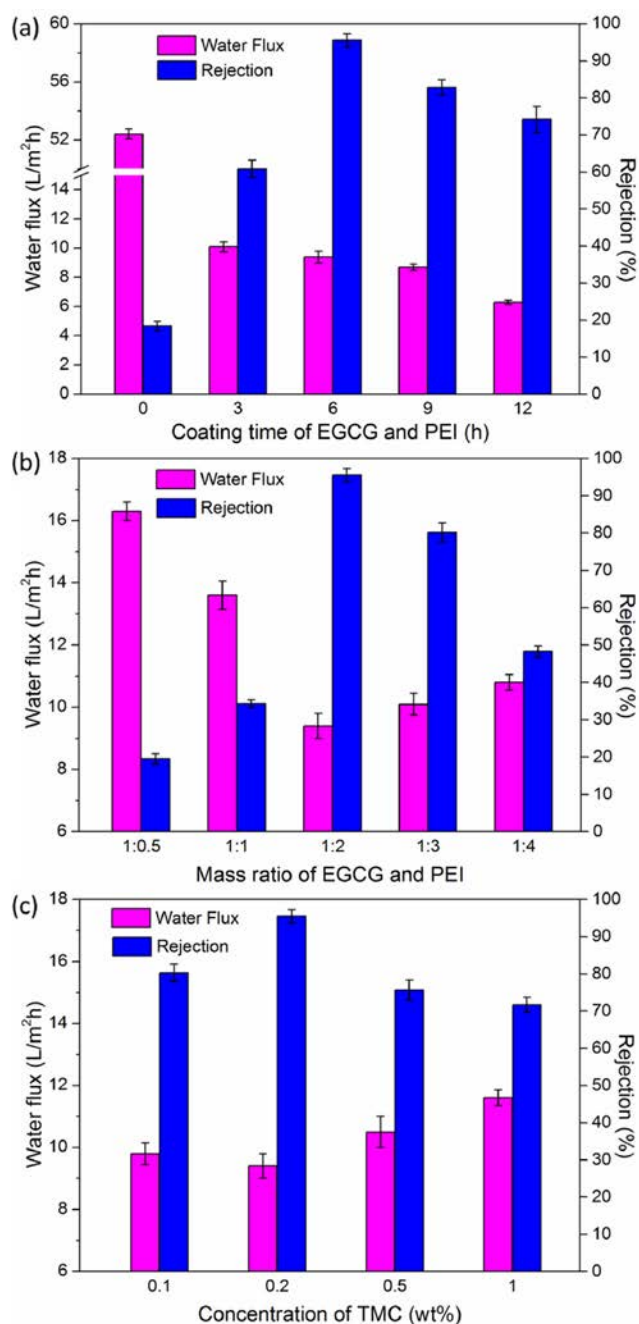


Fig. 6. Effects of (a) EGCG-PEI coating time (EGCG-PEI mass ratio and TMC concentration were fixed at 1:2 and 0.2 wt%, respectively), (b) EGCG-PEI mass ratio (EGCG-PEI coating time and TMC concentration were fixed at 6 h and 0.2 wt%, respectively) and (c) concentration of TMC (EGCG-PEI coating time and EGCG-PEI mass ratio were fixed at 6 h and 1:2, respectively) on the separation performance of the resultant NF membranes. Feed: 1000 mg/L Na₂SO₄ solution at 25 °C. Trans-membrane pressure: 0.2 MPa.

concentration increasing from 1000 mg/L to 5000 mg/L. At high salt concentrations, the excessive salt ions would diffuse on membrane surface to shield the electrostatic repulsion by neutralizing the negative charged surface, leading to lower rejection of anions [40,42]. The result verifies that the salt rejection of charged NF membranes has a dependency on the feed concentration.

Three different types of dye (neutral red, methyl orange and crystal violet) solutions were employed to evaluate dye removal efficiency of the fabricated NF membrane. Dye properties (including molecular weight, molecular volume, diameter, charge and optimized structure)

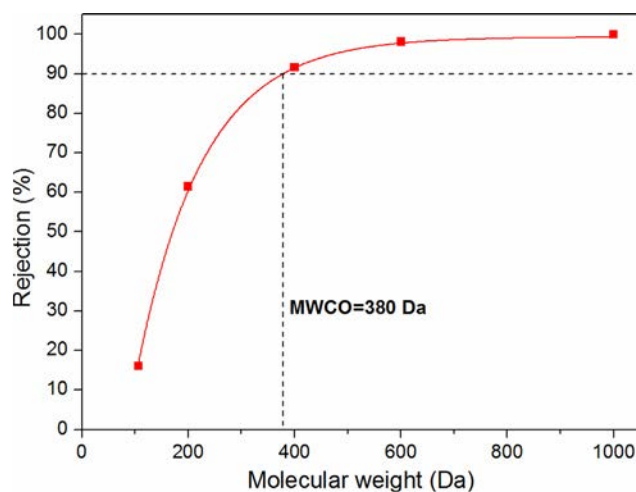


Fig. 7. MWCO of EGCG-PEI-TMC/PTFE.

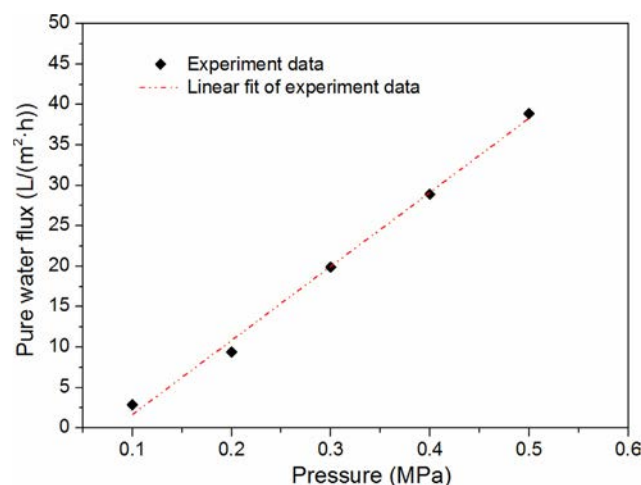


Fig. 8. Effect of operating pressure on pure water flux of EGCG-PEI-TMC/PTFE.

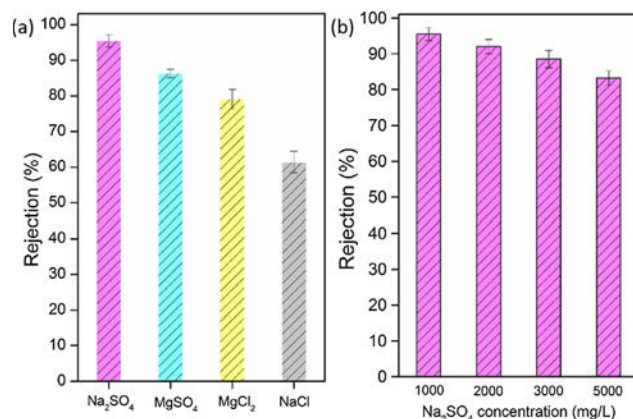


Fig. 9. (a) Separation performance of EGCG-PEI-TMC/PTFE towards four types of salt solutions (salt concentration = 1000 mg/L), (b) the rejection to Na₂SO₄ at different concentrations. Test conditions: 25 °C, 0.2 MPa.

are presented in Table 1. As illustrated in Fig. 10, the membrane exhibits outstanding dye rejections (99.9% for all three dyes) despite of the difference in dye properties. The influence of size exclusion plays a primary role in dye removal due to the large molecular weight of dye molecules [43]. Although the molecular weights of neutral red and methyl orange are smaller than the MWCO (380 Da) of EGCG-PEI-TMC/

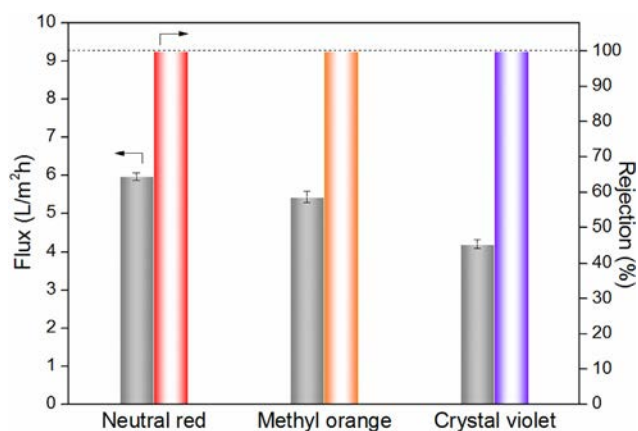


Fig. 10. Separation performance of EGCG-PEI-TMC/PTFE towards three types of dye solutions (dye concentration = 100 mg/L). Test conditions: 25 °C, 0.2 MPa.

PTFE, the dye molecules could still be excluded by the membrane. The results are reasonable because dye aggregation also plays a role in the separation process. It has been found that dye molecules often exhibit a limited diffusivity and are prone to form large molecules and clusters via inter-molecular hydrogen bonding and/or the hydrophobic interactions between the aromatic rings of adjacent molecules, leading to the increase in actual size of a dye molecule in aqueous solution [25,44,45].

3.5.3. The influence of microporous substrates on membrane performance

In this work, besides hydrophilic PTFE substrates, PES, PVDF and hydrophobic PTFE membranes were selected as porous substrates to fabricate NF membranes as well. The properties including pore size and wettability of the substrates are shown in Table 3. For better comparison, the preparation conditions of all composite NF membranes are identical to those of the optimal membrane (EGCG-PEI-TMC/PTFE). The general applicability of our strategy was demonstrated by the corresponding variations of membrane morphologies as observed by SEM (see Fig. S3), suggesting the successful formation of a top layer on different porous substrate. However, the integrity and uniformity of top layer varied with different substrate, leading to the difference in water flux and rejection properties of the resultant NF membranes, as shown in Table 3. It can be concluded that pore size, pore structure as well as hydrophilicity of porous substrates could significantly affect the cross-linking process, thus influencing membrane separation performance. Notably, hydrophilic PTFE substrate is most suitable for fabricating NF membrane under present conditions.

3.6. Stability of the optimal EGCG-PEI-TMC/PTFE

3.6.1. Structural stability

EGCG-PEI-TMC/PTFE was immersed in absolute ethanol for 14 days to evaluate its structural stability. Fig. 11(a) shows that after 96 h immersion, pure water flux increases from 9.4 L/m²h to 20.8 L/m²h, while

the rejection of Na₂SO₄ decreases by about 27%. The increase in water flux and decrease in salt rejection at the initial stage of immersion might be that a small fraction of EGCG-PEI aggregates and/or polyamide fragments with low molecular weight have dissolved in ethanol, unblocking the membrane pores to some extent [46,47]. However, the pure water flux and rejection for Na₂SO₄ remain almost unchanged from 96 h to 336 h, demonstrating that the membrane structure keeps stable. For comparison, composite NF membrane was also prepared via direct interfacial polymerization of PEI and TMC, assigned as PEI-TMC-EGCG. PEI-TMC-EGCG exhibits satisfying separation properties as shown in Table S1. However, in the long-term ethanol treatment, the water flux of PEI-TMC-EGCG increases steadily while the rejection of Na₂SO₄ decreases sharply as shown in Fig. 11(b), indicating that PEI-TMC-EGCG has much poorer structural stability than EGCG-PEI-TMC/PTFE. The results confirm that the existence of EGCG evidently improves the structural stability of composite NF membrane by enhancing the interaction between active layer and substrate. Notably, the rejections of neutral red for both EGCG-PEI-TMC/PTFE and PEI-TMC/PTFE maintain high during the entire stability test, suggesting that ethanol treatment could swell polymeric membrane but not seriously damage its structure.

3.6.2. Long-term operation stability

To evaluate the long-term operation stability of EGCG-PEI-TMC/PTFE, 120 h continuous filtration of 1000 mg/L Na₂SO₄ solution was carried out. As shown in Fig. 12, there's no obvious degradation in permeate flux during 120 h and Na₂SO₄ rejection can keep about 93.5% after a stable running period, demonstrating that the fabricated NF membrane possesses good durability and long-term stability. It's proposed that the good stability of membrane relies on the good compatibility between membrane selective layer and porous substrate, resulting from the strong adhesion ability of EGCG and the robust interactions among EGCG, PEI and TMC through covalent bindings. It can be seen from Fig. S4 that the morphology and surface chemistry of EGCG-PEI-TMC/PTFE have no apparent variation after being rinsed by pure water for 20 days, demonstrating the robust adhesion and interfacial interactions on the skin layer.

4. Conclusions

In summary, this work opens a simple avenue to construct composite NF membrane with the assistance of polyphenol chemistry for water desalination and reuse. The NF membrane (EGCG-PEI-TMC/PTFE) was successfully prepared via EGCG-PEI co-deposition on porous hydrophilic PTFE substrate followed by TMC cross-linking, as confirmed by ATR-FTIR, XPS, SEM and AFM analysis. The optimal NF membrane prepared at EGCG-PEI coating time of 6 h, EGCG-PEI mass ratio of 1:2 and TMC concentration of 0.2 wt% possessed a defect-free and negatively-charged selective layer with stokes radius of 0.46 nm, which contributed to the desirable rejections of salts (e.g. 95.5% for Na₂SO₄) and superior rejections of dyes (e.g. 99.9% for neutral red). Moreover, the membrane exhibited good structural stability when treated by ethanol as well as good long-term performance stability due to the strong interfacial interaction between the selective layer and

Table 3

Performance of composite NF membranes fabricated with different porous substrates.

Membrane	PWF L/(m ² h)	Rejection (%)		Properties of the substrate	
		Na ₂ SO ₄	Methyl orange	WCA (°)	Pore size (μm)
EGCG-PEI-TMC-PES	35.8 ± 0.4	11.5 ± 1.2	57.6 ± 0.2	49 ± 1	~0.22
EGCG-PEI-TMC-PVDF	1325 ± 32	–	–	124 ± 2	~0.22
EGCG-PEI-TMC-PVDF _{0.1}	27.5 ± 0.5	18.3 ± 1.5	76.4 ± 0.8	110 ± 2	~0.1
EGCG-PEI-TMC-PTFE _{hydrophobic}	9.6 ± 0.7	85.7 ± 0.4	98.6 ± 0.7	143 ± 2	~0.22
EGCG-PEI-TMC-PTFE	9.4 ± 0.4	95.5 ± 1.8	99.9 ± 0.1	52 ± 1	~0.22

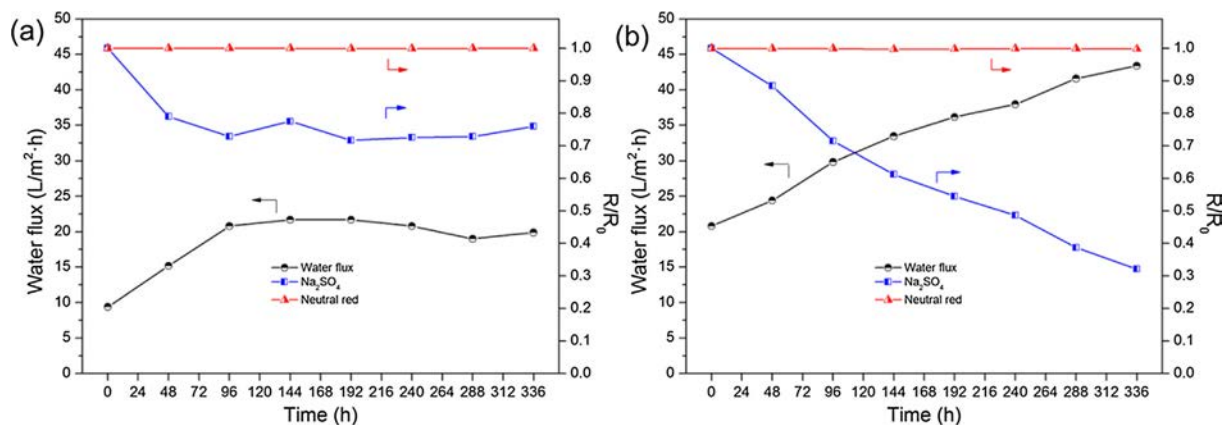


Fig. 11. Effect of ethanol treatment on the performance of (a) EGCG-PEI-TMC/PTFE and (b) PEI-TMC/PTFE. Test conditions: Na₂SO₄ concentration = 1000 mg/L, neutral red concentration = 100 mg/L, 25 °C, 0.2 MPa.

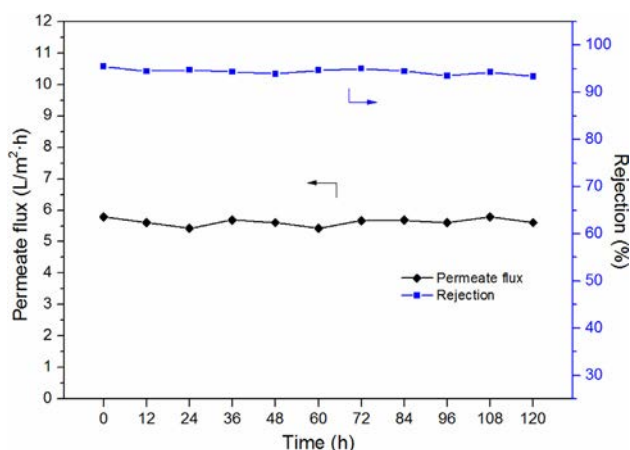


Fig. 12. Long-term stability of EGCG-PEI-TMC/PTFE with different operation time. Test conditions: Na₂SO₄ concentration = 1000 mg/L, 25 °C, 0.2 MPa.

porous substrate. This work broadens the scope of applying polyphenol chemistry in fabricating dense NF membranes to be potentially used in water softening and small organic contaminants removal.

Acknowledgements

We are grateful for the financial support from National Key R&D Program of China (No. 2017YFB0602702-02).

Appendix A. Supplementary material

Supplementary data to this article can be found online at <https://doi.org/10.1016/j.seppur.2019.115964>.

References

- M.M. Mekonnen, A.Y. Hoekstra, Four billion people facing severe water scarcity, *Sci. Adv.* 2 (2016) e1500323.
- J.R. Werber, C.J. Porter, M. Elimelech, A path to ultrasensitivity: support layer properties to maximize performance of biomimetic desalination membranes, *Environ. Sci. Technol.* 52 (2018) 10737–10747.
- S. Chakraborty, M.K. Purkait, S. Dasgupta, S. De, J.K. Basu, Nanofiltration of textile plant effluent for color removal and reduction in COD, *Sep. Purif. Technol.* 31 (2003) 141–151.
- Y. Mansourpanah, E.M. Habibi, Preparation and modification of thin film PA membranes with improved antifouling property using acrylic acid and UV irradiation, *J. Membr. Sci.* 430 (2013) 158–166.
- M. Safarpour, V. Vatanpour, A. Khataee, M. Esmaeili, Development of a novel high flux and fouling-resistant thin film composite nanofiltration membrane by embedding reduced graphene oxide/TiO₂, *Sep. Purif. Technol.* 154 (2015) 96–107.
- Z. Wang, Z. Wang, S. Lin, H. Jin, S. Gao, Y. Zhu, J. Jin, Nanoparticle-templated nanofiltration membranes for ultrahigh performance desalination, *Nat. Commun.* 9 (2018) 2004.
- Y. Lv, H.-C. Yang, H.-Q. Liang, L.-S. Wan, Z.-K. Xu, Nanofiltration membranes via co-deposition of polydopamine/polyethylenimine followed by cross-linking, *J. Membr. Sci.* 476 (2015) 50–58.
- T. Wang, H. Qiblawey, S. Judd, A. Benamor, M.S. Nasser, A. Mohammadian, Fabrication of high flux nanofiltration membrane via hydrogen bonding based co-deposition of polydopamine with poly (vinyl alcohol), *J. Membr. Sci.* 552 (2018) 222–233.
- M. Paul, S.D. Jons, Chemistry and fabrication of polymeric nanofiltration membranes: a review, *Polymer* 103 (2016) 417–456.
- H. Lee, S.M. Dellatore, W.M. Miller, P.B. Messersmith, Mussel-inspired surface chemistry for multifunctional coatings, *Science* 318 (2007) 426–430.
- Y.-L. Ji, M.B.M.Y. Ang, H.-C. Hung, S.-H. Huang, Q.-F. An, K.-R. Lee, J.-Y. Lai, Bio-inspired deposition of polydopamine on PVDF followed by interfacial cross-linking with trimesoyl chloride as means of preparing composite membranes for isopropanol dehydration, *J. Membr. Sci.* 557 (2018) 58–66.
- X.Q. Cheng, C. Zhang, Z.X. Wang, L. Shao, Tailoring nanofiltration membrane performance for highly-efficient antibiotics removal by mussel-inspired modification, *J. Membr. Sci.* 499 (2016) 326–334.
- F.-Y. Zhao, Y.-L. Ji, X.-D. Weng, Y.-F. Mi, C.-C. Ye, Q.-F. An, C.-J. Gao, High-flux positively charged nanocomposite nanofiltration membranes filled with poly (dopamine) modified multiwall carbon nanotubes, *ACS Appl. Mater. Interf.* 8 (2016) 6693–6700.
- C. Wang, Z. Li, J. Chen, Y. Yin, H. Wu, Structurally stable graphene oxide-based nanofiltration membranes with bioadhesive polydopamine coating, *Appl. Surf. Sci.* 427 (2018) 1092–1098.
- A. Sánchez-Rivera, S. Corona-Avendano, G. Alarcón-Angeles, A. Rojas-Hernández, M. Ramirez-Silva, M. Romero-Romo, Spectrophotometric study on the stability of dopamine and the determination of its acidity constants, *Spectrochim. Acta* 59 (2003) 3193–3203.
- T.S. Sileika, D.G. Barrett, R. Zhang, K.H.A. Lau, P.B. Messersmith, Colorless multifunctional coatings inspired by polyphenols found in tea, chocolate, and wine, *Angew. Chem.* 125 (2013) 10966–10970.
- Z. Huang, P. Delparastan, P. Burch, J. Cheng, Y. Cao, P.B. Messersmith, Injectable dynamic covalent hydrogels of boronic acid polymers cross-linked by bioactive plant-derived polyphenols, *Biomater. Sci.* 6 (2018) 2487–2495.
- J. Guo, Y. Ping, H. Ejima, K. Alt, M. Meissner, J.J. Richardson, Y. Yan, K. Peter, D. Von Elverfeldt, C.E. Hagemeyer, Engineering multifunctional capsules through the assembly of metal-phenolic networks, *Angew. Chem. Int. Edit.* 53 (2014) 5546–5551.
- H. Ejima, J.J. Richardson, K. Liang, J.P. Best, M.P. van Koevreden, G.K. Such, J. Cui, F. Caruso, One-step assembly of coordination complexes for versatile film and particle engineering, *Science* 341 (2013) 154–157.
- W.-Z. Qiu, G.-P. Wu, Z.-K. Xu, Robust coatings via catechol-amine codeposition: mechanism, kinetics, and application, *ACS Appl. Mater. Interf.* 10 (2018) 5902–5908.
- M.H. Abdellah, L. Pérez-Manríquez, T. Puspasari, C.A. Scholes, S.E. Kentish, K.-V. Peinemann, A catechin/cellulose composite membrane for organic solvent nanofiltration, *J. Membr. Sci.* 567 (2018) 139–145.
- F. You, Y. Xu, X. Yang, Y. Zhang, L. Shao, Bio-inspired Ni²⁺-polyphenol hydrophilic network to achieve unconventional high-flux nanofiltration membranes for environmental remediation, *Chem. Commun.* 53 (2017) 6128–6131.
- N. Zhang, B. Jiang, L. Zhang, Z. Huang, Y. Sun, Y. Zong, H. Zhang, Low-pressure electroneutral loose nanofiltration membranes with polyphenol-inspired coatings for effective dye/divalent salt separation, *Chem. Eng. J.* 359 (2019) 1442–1452.
- Y. Chen, F. Liu, Y. Wang, H. Lin, L. Han, A tight nanofiltration membrane with multi-charged nanofilms for high rejection to concentrated salts, *J. Membr. Sci.* 537 (2017) 407–415.
- J. Lin, W. Ye, M.-C. Baltaru, Y.P. Tang, N.J. Bernstein, P. Gao, S. Balta, M. Vlad, A. Volodin, A. Sotto, Tight ultrafiltration membranes for enhanced separation of

- dyes and Na₂SO₄ during textile wastewater treatment, *J. Membr. Sci.* 514 (2016) 217–228.
- [26] G. Liu, Z. Jiang, C. Chen, L. Hou, B. Gao, H. Yang, H. Wu, F. Pan, P. Zhang, X. Cao, Preparation of ultrathin, robust membranes through reactive layer-by-layer (LbL) assembly for pervaporation dehydration, *J. Membr. Sci.* 537 (2017) 229–238.
- [27] S. Quideau, D. Deffieux, C. Douatcasassus, L. Pouysegu, Plant polyphenols: chemical properties, biological activities, and synthesis, *Angew. Chem.* 50 (2011) 586–621.
- [28] Y.C. Xu, Y.P. Tang, L.F. Liu, Z.H. Guo, L. Shao, Nanocomposite organic solvent nanofiltration membranes by a highly-efficient mussel-inspired co-deposition strategy, *J. Membr. Sci.* 526 (2017) 32–42.
- [29] X. Zhao, N. Jia, L. Cheng, L. Liu, C. Gao, Metal-polyphenol coordination networks: towards engineering of antifouling hybrid membranes via in situ assembly, *J. Membr. Sci.* 563 (2018) 435–446.
- [30] J. Zhao, C. Fang, Y. Zhu, G. He, F. Pan, Z. Jiang, P. Zhang, X. Cao, B. Wang, Manipulating the interfacial interactions of composite membranes via a mussel-inspired approach for enhanced separation selectivity, *J. Mater. Chem. A* 3 (2015) 19980–19988.
- [31] C.Y. Tang, Y.-N. Kwon, J.O. Leckie, Effect of membrane chemistry and coating layer on physicochemical properties of thin film composite polyamide RO and NF membranes: I. FTIR and XPS characterization of polyamide and coating layer chemistry, *Desalination* 242 (2009) 149–167.
- [32] S. Zhang, Z. Jiang, X. Wang, C. Yang, J. Shi, Facile method to prepare microcapsules inspired by polyphenol chemistry for efficient enzyme immobilization, *ACS Appl. Mater. Interf.* 7 (2015) 19570–19578.
- [33] Y. Tian, Y. Cao, Y. Wang, W. Yang, J. Feng, Realizing ultrahigh modulus and high strength of macroscopic graphene oxide papers through crosslinking of mussel-inspired polymers, *Adv. Mater.* 25 (2013) 2980–2983.
- [34] W.-Z. Qiu, H.-C. Yang, L.-S. Wan, Z.-K. Xu, Co-deposition of catechol/polyethyleneimine on porous membranes for efficient decolorization of dye water, *J. Mater. Chem. A* 3 (2015) 14438–14444.
- [35] M.B.M.Y. Ang, Y.-L. Ji, S.-H. Huang, H.-A. Tsai, W.-S. Hung, C.-C. Hu, K.-R. Lee, J.-Y. Lai, Incorporation of carboxylic monoamines into thin-film composite polyamide membranes to enhance nanofiltration performance, *J. Membr. Sci.* 539 (2017) 52–64.
- [36] X. Su, H. Li, X. Lai, Z. Yang, Z. Chen, W. Wu, X. Zeng, Vacuum-assisted layer-by-layer superhydrophobic carbon nanotube films with electrothermal and photo-thermal effects for deicing and controllable manipulation, *J. Mater. Chem. A* 6 (2018) 16910–16919.
- [37] X. Wang, Y. Fang, C. Tu, B. Van der Bruggen, Modelling of the separation performance and electrokinetic properties of nanofiltration membranes, *Int. Rev. Phys. Chem.* 31 (2012) 111–130.
- [38] J. Cheng, W. Shi, L. Zhang, R. Zhang, A novel polyester composite nanofiltration membrane formed by interfacial polymerization of pentaerythritol (PE) and trimethylolpropane trimethyl ether (TM), *Appl. Surf. Sci.* 416 (2017) 152–159.
- [39] X. Li, Y. Cao, H. Yu, G. Kang, X. Jie, Z. Liu, Q. Yuan, A novel composite nanofiltration membrane prepared with PHGH and TMC by interfacial polymerization, *J. Membr. Sci.* 466 (2014) 82–91.
- [40] R. Huang, G. Chen, M. Sun, Y. Hu, C. Gao, Studies on nanofiltration membrane formed by diisocyanate cross-linking of quaternized chitosan on poly (acrylonitrile) (PAN) support, *J. Membr. Sci.* 286 (2006) 237–244.
- [41] J. Schaep, B. Van der Bruggen, C. Vandecasteele, D. Wilms, Influence of ion size and charge in nanofiltration, *Sep. Purif. Technol.* 14 (1998) 155–162.
- [42] X. Bai, Y. Zhang, H. Wang, H. Zhang, J. Liu, Study on the modification of positively charged composite nanofiltration membrane by TiO₂ nanoparticles, *Desalination* 313 (2013) 57–65.
- [43] Y. Wang, J. Zhu, G. Dong, Y. Zhang, N. Guo, J. Liu, Sulfonated halloysite nanotubes/polyethersulfone nanocomposite membrane for efficient dye purification, *Sep. Purif. Technol.* 150 (2015) 243–251.
- [44] K. Hamada, H. Nonogaki, Y. Fukushima, B. Munkhbat, M. Mitsuishi, Effects of hydrating water molecules on the aggregation behavior of azo dyes in aqueous solutions, *Dyes Pigment* 16 (1991) 111–118.
- [45] J. Wang, J. Zhu, M.T. Tsehay, J. Li, G. Dong, S. Yuan, X. Li, Y. Zhang, J. Liu, B. Van der Bruggen, High flux electroneutral loose nanofiltration membranes based on rapid deposition of polydopamine/polyethyleneimine, *J. Mater. Chem. A* 5 (2017) 14847–14857.
- [46] Y.C. Xu, Z.X. Wang, X.Q. Cheng, Y.C. Xiao, L. Shao, Positively charged nanofiltration membranes via economically mussel-substance-simulated co-deposition for textile wastewater treatment, *Chem. Eng. J.* 303 (2016) 555–564.
- [47] A. Kulkarni, D. Mukherjee, W.N. Gill, Flux enhancement by hydrophilization of thin film composite reverse osmosis membranes, *J. Membr. Sci.* 114 (1996) 39–50.